



## Research Article

## Chemically purified cellulose and its nanocrystals from sugarcane baggase: isolation and characterization

Suter K. Evans<sup>a</sup>, Omwoyo N. Wesley<sup>a,b,\*</sup>, Oyaro Nathan<sup>a</sup>, Makwena J. Moloto<sup>b</sup><sup>a</sup> Department of Chemistry, Maasai Mara University, Narok, Kenya<sup>b</sup> Department of Chemistry, Vaal University of Technology, Vanderbijlpark, South Africa

## ARTICLE INFO

## Keywords:

Materials chemistry  
Baggase  
By-product  
Degradation  
Hydrolysis  
Hemicellulose

## ABSTRACT

Agro-wastes such as sugar cane bagasse can be explored for use in different aspects. Its applicability as a source of cellulose has attracted much interests especially in biomedical field among various applications. In the current work chemically purified cellulose (CPC) and cellulose nanocrystals (CNCs) were effectively extracted from sugarcane baggase (SCB). The cellulose was obtained by chemical treatment of SCB using HNO<sub>3</sub>, NaOH and a bleaching agent. Nanocrystals were further prepared from the extracted cellulose using H<sub>2</sub>SO<sub>4</sub> hydrolysis followed by washing with deionized water and acetone. The obtained materials were characterized for surface morphological using Fourier transform infrared (FTIR) spectroscopy, Transmission Electron Microscopy (TEM) and X-ray diffraction (XRD) analysis. The thermal properties were evaluated using TGA/DTG. The FTIR showed the disappearance of the peaks responsible for the hemicelluloses and lignin. These results were confirmed by TGA which proved gradual elimination of non-cellulosic constituents. X-ray Diffractometer depicted an increase in crystallinity occasioned by sequential treatments to get the cellulose nanocrystals. Cellulose nanocrystals had a spherical shape with a diameter of 38nm as compared to the chemically purified cellulose which had a diameter of 76nm. The CNCs prepared with this method were seen to be less agglomerated and more crystalline thus possess a higher potential as bionanocomposite either for biomedical applications or for wastewater treatment among other industrial application. This approach also provides an opportunity for the sugar companies to effectively manage their waste product.

## 1. Introduction

Cellulosic nanomaterials have gained increasing attention as agents for biocomposites for industrial and biomedical applications due to their sustainability and renewability (Faruk et al., 2012). Their surfaces are rich with (-OH) groups that can be chemically modified (Plackett, 2010). They are characterized with low density, high aspect ratio, good mechanical features and faint toxicity (Lavoine et al., 2012). Several studies on nanomaterials has been extensively done for an extensive potential use; scaffolds for tissue engineering, filters, membranes for water treatment, transparent films, adhesives, drug delivery and antimicrobial films, among other uses (Moon et al., 2011). Cellulose is a natural water permeable agro-based polymer comprised hydroxyl functional groups that enhance the hydrogen bonding. Cellulose can be obtained from cotton, sisal, *Phormium tenax* leaf fibers, corncob, banana rachis, rice

husk, soy hulls, cassava baggase and sugarcane baggase (Kumar et al., 2014). Research studies on the use of cellulosic waste for various functions have grown rapidly. Crystalline cellulose has been previously been extracted from cornstalks (Reddy and Yang, 2005), cassava baggase (Pasquini et al., 2010), coconut husk (Rosa et al., 2010), banana rachis (Zuluaga et al., 2009), soybean pods (Wang and Sain, 2007), mulberry bark (Li et al., 2009), wheat and soy hulls (Alemdar and Sain, 2008, Johar and Dufresne, 2012). Other major components of plants include hemicelluloses and lignin. Lignin is more of a cementing-matrix for cellulose and hemicellulose with Ester-type bond linkage that is both very sensitive and insensitive to alkali treatments. The cellulosic materials are known to be crystalline while lignin and hemicellulose are reported to be amorphous (Kumar et al., 2014). Cellulosic materials can be classified into cellulose nanocrystals (CNCs) and cellulose nanofibrils (CNFs) which can also be referred as nanofibrillated cellulose (NFC) or microfibrillated

\* Corresponding author.

E-mail address: [wesleyomwoyo@mmarau.ac.ke](mailto:wesleyomwoyo@mmarau.ac.ke) (O.N. Wesley).<https://doi.org/10.1016/j.heliyon.2019.e02635>

Received 22 July 2019; Received in revised form 29 August 2019; Accepted 8 October 2019

2405-8440/© 2019 The Authors. Published by Elsevier Ltd. This is an open access article under the CC BY-NC-ND license (<http://creativecommons.org/licenses/by-nc-nd/4.0/>).

cellulose (MFC) depending on their size and extraction method (Kumar et al., 2014).

Cellulosic nanomaterials have been used to prepare composites with higher mechanical strength (Lu and Hsieh, 2010). Cellulose nanofibrils have been used as carriers for delivery of drugs (Johar et al., 2012) among many other applications. The major challenge of preparing the cellulose nanocrystals for further applications is their tendency to aggregate. The hydrogen bonds of cellulose pull the cellulose nanocrystals together and make their re-dispersion difficult thus hindering their effective processing (Kumar et al., 2014). Various methods have been used to prepare cellulose nanocrystals which include ultrasonic technique, acid hydrolysis, and enzymatic hydrolysis (Mashego, 2016) though the acid hydrolysis has been mostly used since the method is simple and fast to generate cellulose nanocrystals. In other studies cellulose nanofibrils were prepared from bagasse pulp through ultra-micron grinding and high pressure homogenization using xylanase enzyme and cold alkali for pre-treatment (Nie et al., 2018; Tao et al., 2019). It is therefore necessary to develop suitable methods to isolate the cellulose nanocrystals that will be free from aggregation and Ostwald ripening.

There are several agro-based industries that produce huge amounts of plant biomass. Sugarcane is the world's largest crop by production quantity, with approximately 1.9 billion tonnes produced yearly (Otieno, 2015). In Kenya Sugarcane is mainly grown in the former western and Nyanza provinces. The industry has eleven operational sugar factories namely, Chemelil Sugar Factory; Kibos Sugar and Allied Factories; Muhoroni Sugar Factory; Mumias Sugar Factory; Nzoia Sugar Factory; Soin Sugar Factory; South Nyanza Sugar Factory; Sukari Industries Limited; Transmara Sugar Factory; West Kenya Sugar Factory and Butali Sugar Factory (Otieno, 2015). Sugarcane bagasse is an agro-based dry pulpy residue after the extraction of juice from cane from these industries. Bagasse has been reported to cause tremendous environmental pollution in the areas located with sugar industries since they are scattered all over making the scenery of these areas to look ugly. The bagasse wastes produce bad odors when it ferments making the environment not conducive to reside on. Furthermore, these wastes cost the industries on storage space and disposal costs. The sugar industries generate huge quantity of bagasse during the manufacture of sugar from cane. This phenomenon results to environmental distress, also triggering numerous environmental extortions instigating damage to the land and its surroundings (Masayi and Netondo, 2012). Diverse methods for bagasse disposal, including using it for power co-generation and manufacture of molasses which is used for industrial production of ethanol have been explored by the factories. The sugarcane bagasse has also been explored for the manufacture of briquettes though all this use has not addressed the menace of bagasse (Otieno, 2015). Other uses of sugarcane bagasse comprise exploitation of its cellulose content (Jacobsen and Wyman, 2000) for further application either in water treatment or other relevant uses to the very industries or for sale. Thus, the extraction of cellulose from sugarcane bagasse for the production of cellulose nanocrystals was sought.

Therefore this study explored the extraction of cellulose from sugarcane bagasse and to isolate cellulose nanocrystals from the prepared cellulose. The raw bagasse, chemically purified cellulose and the cellulose nanocrystals were characterized for surface morphology using TEM, and FTIR, crystallinity analysis using XRD and thermal properties using TGA.

### 1.1. Statement of hypothesis

Extraction of cellulose from sugarcane bagasse can be enhanced by the use of nitric acid as a starting material for digestion. Cellulose nanocrystals can further be prepared from extracted cellulose for enhanced properties and applications.

## 2. Materials and methods

### 2.1. Materials

The Sugarcane bagasse which is an agricultural waste was collected from South Nyanza Sugar Company, Awendo, Kenya (Sony Sugar Company). Nitric acid  $\text{HNO}_3$  ( $\geq 98.99\%$ ), Sodium hypochlorite ( $\text{NaClO}$ ), Sulfuric acid  $\text{H}_2\text{SO}_4$  ( $\geq 99.9\%$ ), acetic acid, sodium hydroxide and acetone ( $\geq 99.9\%$ ) were used and were of analytical grade. Deionized water was used all through the entire experiment.

### 2.2. Methods

#### 2.2.1. Isolation of chemically purified cellulose

Sugarcane bagasse was primarily washed with deionized water to remove any unwanted particles. It was then sun-dried before grinding into small pieces using a blender and sieved under double mesh sieves. The powdered bagasse was oven dried at  $105^\circ\text{C}$  for about 5 h and then stored at room temperature in air tight polythene bags. The isolation of the cellulose was done according to previously documented methods (Johar et al., 2012) but with some modifications. Briefly, 70 g of the bagasse powder was mixed with 700 mL 6% (w/v) of  $\text{HNO}_3$  for 2 h in a hot water bath placed at  $80^\circ\text{C}$  then washed with deionized water until neutral. The solution was then refluxed with 500 mL of 1% NaOH at constant stirring for 2 h at  $80^\circ\text{C}$  in a hot water bath. It was further washed with deionized water and bleached with 250mL of sodium hypochlorite 0.735% (w/v). Acetic acid was further added to the ligno-cellulosic extract and stirred for 2 h at  $80^\circ\text{C}$ . The residue was then washed with deionized water until a neutral pH and left to dry for three days at room temperature.

#### 2.2.2. Preparation of cellulose nanocrystals (CNCs)

The isolated cellulose was used to prepare cellulose nanocrystals by hydrolysis as described in literature (Kumar et al., 2014) though with slight modifications also. The chemically CPC from SCB was hydrolyzed with 32% (w/v) of  $\text{H}_2\text{SO}_4$  with a 1:25 g/mL ratio of cellulose to the dilute acid at room temperature for 24 h under constant stirring. This reaction was then quenched by addition of 10 fold deionized water to the reaction mixture, followed by centrifugation at 10,000 rpm for 15 min three times to remove the acidic solution. The supernatant was discarded and the cellulosic precipitate re-dispersed in deionized water and dialyzed against deionized water several times. The colloidal suspension was then sonicated in an ice bath sonicator for 1 h to homogenize the generated cellulose nanocrystals. The generated nanocrystals were further centrifuged at 6,000 rpm for 30 min. This was then allowed to settle for 24 h then the water was replaced with acetone and centrifuged at 6,000 rpm for 30 min. The cellulose nanocrystals were finally oven dried in vacuum at  $70^\circ\text{C}$  overnight.

### 2.3. Characterization of SCB, CPC and CNCs

#### 2.3.1. Fourier transform infrared spectroscopy (FTIR)

This technique was used to manipulate structural changes on samples as a result of chemical modification by the identification of the functional groups. The changes in functional groups of the materials; SCB, CPC and CNCs were investigated using FTIR spectroscopy using Nicolet, iS50, FT-IR (Thermo Nicolet, USA) spectrophotometer. The FTIR spectra of the samples were recorded in the transmittance mode in the range of  $4000\text{ cm}^{-1}$  to  $500\text{ cm}^{-1}$ .

#### 2.3.2. Transmission Electron Microscopy (TEM)

Morphological properties and particle sizes of CPC and CNCs were determined using (Tecnaï G2 20 S-twin) Transmission Electron Microscope. The samples were dispersed in a suitable medium and then placed on a copper grid coated with a carbon film. Thereafter, the samples were then dried before carrying out TEM analysis at an accelerating voltage of

100–120 kV.

### 2.3.3. X-ray diffraction (XRD)

The crystallinity index of the SCB before and after chemical modification was analyzed using Shimadzu XRD-700 X-RAY Diffractometer. SCB, CPC and CNCs in form of milled powder were placed on steel sample holders and leveled to obtain total and uniform X-ray exposure. The samples were analyzed at 25 °C with a monochromatic CuK $\alpha$  radiation source  $\lambda = 0.1539$  nm with a 2 theta angle ranging from 10° to 60°. The crystallinity index was calculated using the equation below (Johar et al., 2012).

$$C_r I(\%) = \frac{I_{002} - I_{am}}{I_{002}} \times 100$$

Where,  $I_{002}$  denotes the maximum intensity of the 002 lattice diffraction peak and  $I_{am}$  is the minimum intensity scattered by the amorphous part of the sample (Johar et al., 2012).

### 2.3.4. Thermogravimetric analysis (TGA)

To confirm the removal of hemicellulose and lignin, TGA measurements were performed for SCB, CPC and CNCs using a Mettler Toledo thermogravimetric analyzer (TGA/SDTA 85-F). Under all measurements a mass of 12 mg was used in each analysis. In addition, the thermal measurements were carried out with a gas flow rate of 10 mL min<sup>-1</sup> heating from 30 °C to 900 °C under nitrogen atmosphere.

## 3. Results and discussions

### 3.1. Physical appearances

The physical appearances of the raw sugarcane bagasse that was collected from the factory, the powdered bagasse, the chemically purified cellulose and its nanocrystals prepared by hydrolysis method are captured below in Fig. 1. The color of the raw bagasse whitened as a result of the chemical modification. As shown in Fig. 1, the raw sugarcane bagasse and its powdered form had a brown color. The treatment of the bagasse with HNO<sub>3</sub>, NaOH and sodium hypochlorite changed the texture of the powder and also changed the color to white (Fig. 1c) when the cellulose was formed. This degradation process was observed through the loss of weight of the starting material and the disappearance of some functional groups as evident from the TGA and FTIR data respectively. The hydrolysis of the extracted cellulose with H<sub>2</sub>SO<sub>4</sub> acid and finally washing with acetone produced the nanocrystals that were whiter and finer by texture (Fig. 1d). Similar results were obtained by Chieng et al. (2017), who studied the extraction and characterization of cellulose nanocrystals from Oil palm Mesocarp fiber (OPMF). This study found that raw Oil palm Mesocarp fiber changed its color when chemically treated especially with the bleaching agent. His results indicated that the bleaching agent produced fibers that were relatively white in color. In other studies, Johar et al. (2012), visualized and characterized physical and chemical properties of rice husks fibers while treating them at different stages. The color of the untreated rice husk was brown and turned brown during treatment with an alkaline solution, the material

appeared completely white in color after bleaching. Studies have attributed the color changes to the removal of hemicellulose, lignin and other impurities after treatment (Bledzki et al., 2010).

### 3.2. Fourier transform infrared (FTIR) spectroscopy analysis

The structural change of the SCB was determined by FTIR before and after chemical treatment. The Infra-Red spectra of SCB, CPC and the CNCs are captured below in Fig. 2. The broad peak at 3100–3500 cm<sup>-1</sup> indicates the O–H stretching bonds while the peak around 2800–2950 cm<sup>-1</sup> indicates the C–H stretching. The peak around 1750 cm<sup>-1</sup> corresponds to C=O bond which is normally found in the linkages of the esters in the hemicellulose and lignin. The peaks observed around 1600–1700 cm<sup>-1</sup> indicates the aromatic ring found in the lignin. The peak between 1200–1300 cm<sup>-1</sup> depicts an out of plane C–O stretching in the aryl group of the lignin linked to the SCB before chemical modification. The modification of SCB with sodium chloride and sodium hypochlorite lead to the disappearance the bands, FTIR spectrum of CPC and CNCs (Fig. 2). The outcome of this chemical treatment can be noted from the main spectral bands which must be emphasized between 1500–1600 cm<sup>-1</sup> and around 1250 cm<sup>-1</sup>. The two spectral bands in these positions are seen to disappear after the chemical treatments to form the CPC and CNCs (Johar et al., 2012). The FTIR spectrum of CNCs is similar to that of CPC but it has sharp bands. The peaks observed at 1600–1650 cm<sup>-1</sup> for the CPC and CNCs are as a result of O–H bending due to adsorbed water (Johar et al., 2012), the bands between 1400–1450 cm<sup>-1</sup> is attributed to CH<sub>2</sub> intertwined in the cellulosic material. The peak at 1050 cm<sup>-1</sup> indicates the C–O–C pyranose ring stretching vibration (R. Liu, Yu and Huang, 2005). The peak observed around 900 cm<sup>-1</sup> is reported to be associated with the cellulosic  $\beta$ -glycosidic linkages (Reddy and Yang, 2005). These results depicted that the cellulose molecular structure remains unaffected following chemical treatment of SCB.

### 3.3. X-ray diffraction (XRD) analysis

The X-ray diffraction patterns of the SCB, CPC and CNCs are shown below in Fig. 3. The crystallinity index of SCB, CPC and CNCs was calculated from the XRD. Crystallinity index (CrI) denotes the ratio of the crystalline constituents to the amorphous regions of a material (Kumar et al., 2014). The SCB, CPC and CNCs exhibited three main characteristic peaks around a 2 $\theta$  value of 16.1°, 22.1° and 37.5°. The peaks represents the characteristic patterns for the crystal form of cellulose I polymorph since there is no doublet peak around 2 $\theta$  value of 22° (Klemm et al., 2005). The peak at 2 $\theta$  value 16.1° corresponds to (110) crystallographic plane while the one at 2 $\theta$  value of 22.1° and 37.5° relate to the (002) and (004) crystallographic planes correspondingly (Johar et al., 2012). After the treatment, more intense crystalline peaks were observed with the main reflections at 2 $\theta$  value of 22.1° and 37.5°. This was also a confirmation of the successful removal of the lignin from the bagasse. The samples presented high peak intensity around 2 $\theta$  value of 22.1° which is correlated to the crystalline structure of cellulose. Also, from the XRD patterns, presence of a broad peak at 2 $\theta$  around 16° is characteristic to the amorphous arrangement.



Fig. 1. Physical appearance of collected sugarcane bagasse (a), crushed sugarcane bagasse (b), extracted cellulose (c) and nanocrystals (d).

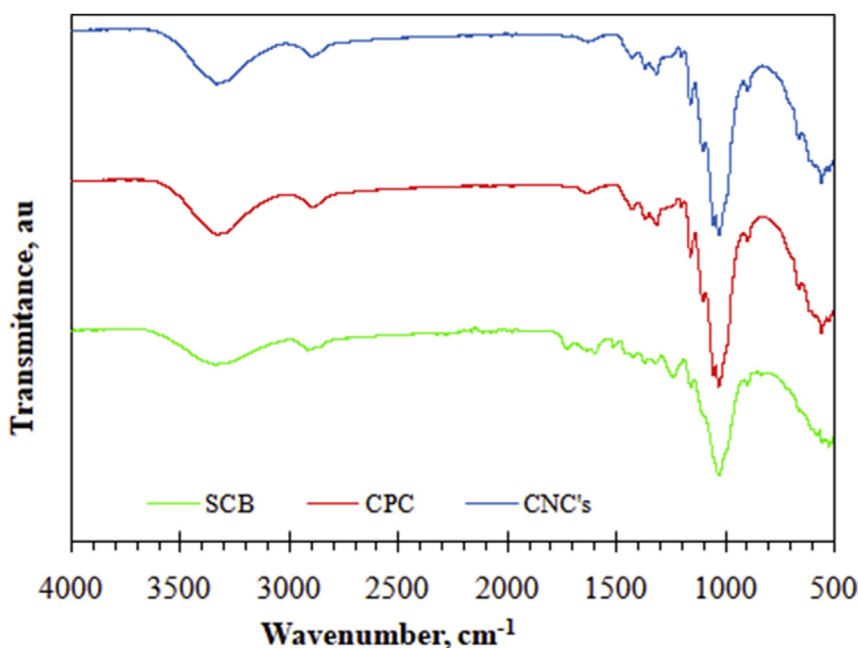


Fig. 2. FTIR spectra for SCB, CPC and CNCs.

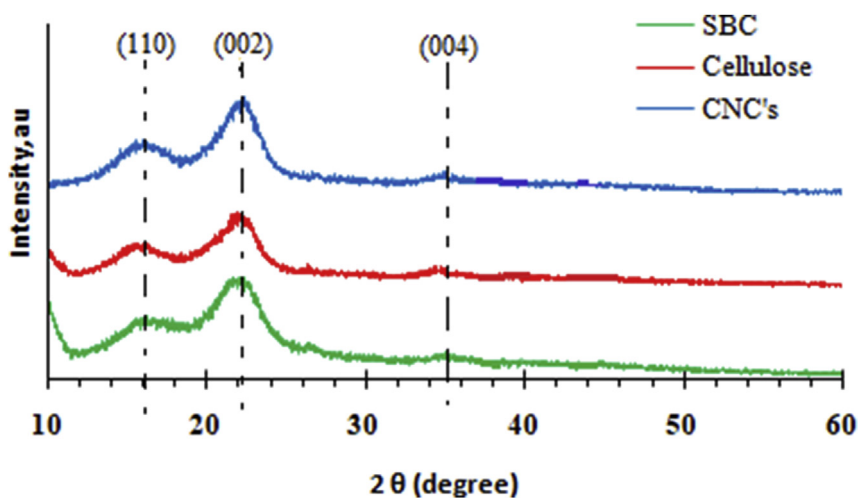


Fig. 3. X-ray diffraction patterns of SCB, CPC and CNCs.

The crystallinity index (CrI) of SCB to CPC to CNCs that were calculated for the XRD patterns presented an increase in crystallinity SCB > CPC > CNCs (Table 1). From the experimental data SCB presented the lowest CrI due to higher amounts of the amorphous constituents. With chemical modification using sodium hydroxide and sodium hypochlorite in extraction of the cellulose, crystallinity increased. This is attributed to successful elimination of hemicelluloses and lignin that were attached to the cellulosic bagasse. Crystallinity index was observed to increase from

**Table 1**  
Crystallinity index of SCB, CPC and CNCs.

Sample	$2\theta$ (Amorphous) (°)		$2\theta$ (002) (°)		Crystallinity Index (CrI%)
	Degree	Intensity, $I_{am}$	Degree	Intensity, $I_{002}$	
SCB	16.34	394	22.28	664	40.66
CPC	16.12	292	22.38	892	67.26
CNCs	16.32	214	22.34	926	76.89

SCB to CPC after acid hydrolysis using sulfuric acid. The increase in crystallinity upon acid hydrolysis depicted the dissolution of the amorphous region of the SCB. During the chemical treatment, sulfuric acid reacts with the amorphous region of SCB causing hydrolytic cleavage of the glycosidic bonds thus releasing individual crystallites. This in turn causes the growth of monocrystals which contributes to the increase in crystallinity which is observed as narrow and pronounced diffraction peaks in the XRD curve. Similar results were obtained by Johar et al. (2012), where they extracted cellulose nanocrystals from rice husks. Their untreated rice husks and the treated ones showed characteristic peaks typical of cellulose I with three well defined crystalline peaks around  $2\theta$  value of  $16^\circ$ ,  $22^\circ$  and  $35^\circ$ . The peaks equally became more defined upon each step of chemical treatment. In other studies, similar patterns were observed when the cellulose nanocrystals was extracted by chemical treatments of other agricultural wastes including from wheat straw (Liu et al., 2005), from oil palm mesocarp fiber (Chieng et al., 2017), from corn Stover (Costa et al., 2015) and even from Agave

*angustifolia* fiber (Rosli et al., 2013).

In all these studies, the crystallinity of cellulose increased with further chemical treatments. The crystallinity of cellulose is important in the determination of thermal stability, elasticity, sorption efficiency and more physical features which are of essence for industrial applications. Increased crystallinity increases the rigidity and stiffness of a substance and therefore increasing its strength. This in turn enables the production of nanocomposites with enhanced mechanical properties (Alemdar and Sain, 2008). The method used herein for the production of CNCs, gave slightly higher values of crystallinity compared to other studies.

### 3.4. Thermogravimetric analysis

The thermal property of any given sample is an essential feature in the determination of the response to a mass change with respect to temperature. Thermogravimetric (TG) curves displayed weight variations under heating with respect to the derivative curve displaying differences in the TG slope that cannot be easily noted with TGA curve. From the DTG curves differences in temperature can indicate on whether the thermal process is exothermic or endothermic. The TGA and DTG thermal properties of the baggase, extracted cellulose and the nanocrystals are shown in Fig. 4 below. This was performed to investigate the suitability of SCB and the cellulosic compounds. The thermal behavior of the lignocellulosic materials depends on their chemical composition, structure and degree of crystallinity (Rosli et al., 2013). The thermal decomposition parameters were determined from TGA as shown in the graphs. The TGA curve for the SCB showed four degradation steps which are characteristic of moisture content, hemicellulose, cellulose and lignin degradation. The initial weight loss started at about 40 °C for the three samples and this went on until a maximum temperature ( $T_{max}$ ) of 128 °C. This degradation was attributed to the loss of moisture content of the samples. The graphs depict that CPC had the highest moisture content of around 8% while the SCB and CNCs has a moisture content of about 3% each. The second degradation step for SCB starts around 200 °C which is a starting temperature for the lignin degradation.

The lignin decomposes very slowly over a broader range of temperature (200–800 °C) than the cellulose and hemicellulose components of the biomass (Brebú and Vasile, 2010). Previous studies have documented DTG curves of lignin decomposition as having flat peaks with a sloping baseline which makes it impossible to define activation energy for the reaction since there is a flat tailing section at higher temperatures (H. Liu, Liu et al., 2010). This phenomenon is different for the sharper and pronounced DTG peaks of cellulose and hemicellulose. Brebú and Vasile (2010) explained the non existence of the degradation peak responsible

for lignin. Since the heating rate is 10 °C/min and the lignin decomposes very slowly at approximately less than 0.15 wt%/°C, the mass lost is only 40 wt% of its initial mass below 700 °C. The degradation rate then slightly increases to 0.3 wt%/°C above 750 °C and finally the mass loss at around 850 °C is documented to be approximately 67 wt% (Yang et al., 2006). The degradation for SCB recorded between (204–300 °C) with a  $T_{max}$  around 280 °C is attributed to the degradation of hemicelluloses (Rosli et al., 2013). The degradation peak observed at a  $T_{max}$  around 350 °C in the SCB curve is attributed to the cellulose degradation. The degradation of the CPC occurred in the range of 224–357 °C with a  $T_{max}$  observed at about 320 °C while the CNCs degraded in the range of 240–341 °C with a  $T_{max}$  around 310 °C.

Generally, the degradation temperature is seen to decrease when the SCB is chemically treated and hydrolyzed. This is attributed to the removal of hemicelluloses and lignin as well as the crystallinity of the CPC and CNCs which is higher than SCB. Basically, increase in crystallinity is documented to improve heat resistance and this leads to an improvement in the thermal stability of a material (Rosli et al., 2013). The further reduction of the degradation temperature of the CNCs may also be attributed to the introduction of the sulfate groups into the cellulose crystals during the sulfuric acid hydrolysis process (Lavoine et al., 2012). The residue left after complete degradation of the samples were observed to be about 19.6% for the SCB while CPC and CNCs had only 14.8% left for each. The higher residual amounts recorded for SCB is attributed to the presence of lignin which as earlier said, have a very slow degradation rate and might not be completely burnt (Johar et al., 2012). The amounts of residue recorded for CPC and CNCs are slightly lower signifying the successful removal of the lignin (Rosli et al., 2013).

### 3.5. Transmission Electron Microscopy

Transmission Electron microscopy was used to study the morphology and determine the particle sizes of the chemically purified cellulose and cellulose nanocrystals. The chemical treatment of the SCB with an alkali solution and further by acid hydrolysis was expected to remove the hemicelluloses and lignin which form part of the amorphous region of the cellulosic baggase (Ahmed et al., 2005). This process is aimed at reducing the size of the cellulosic nanomaterials to nanometer range while leaving the crystalline regions intact. Micrographs from the TEM analysis of CPC and their mean particle size is shown in Fig. 5 while that of CPC is shown in Fig. 6.

The CPC had an average size of 76 nm in comparison to that of CNCs with 38nm average particle size. From the TEM image of CPC, it can be observed that the particles are having short 'rod like' shapes which have

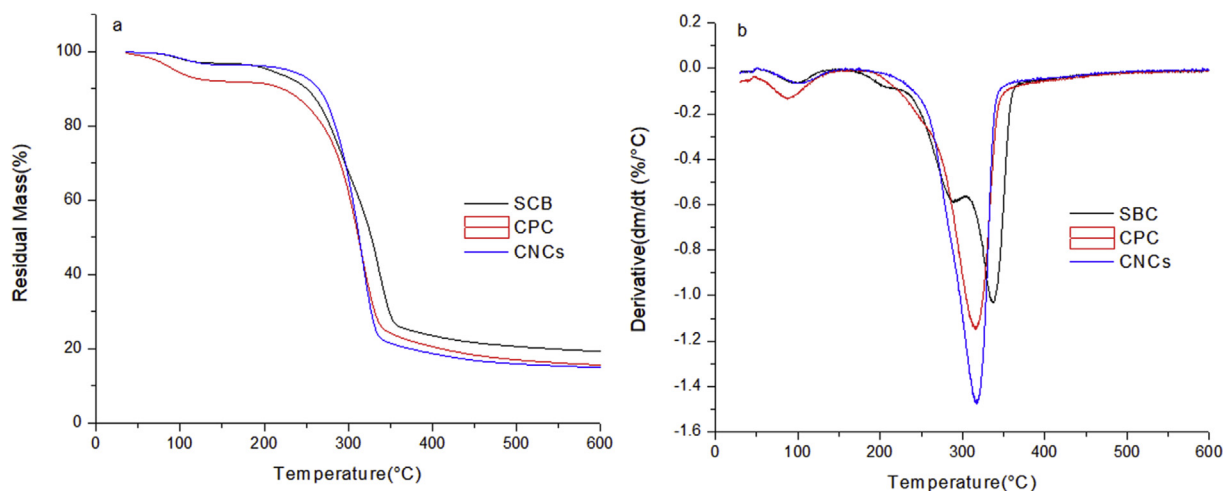


Fig. 4. TGA(a) and TDG (b) curves of SCB, CPC and CNCs.

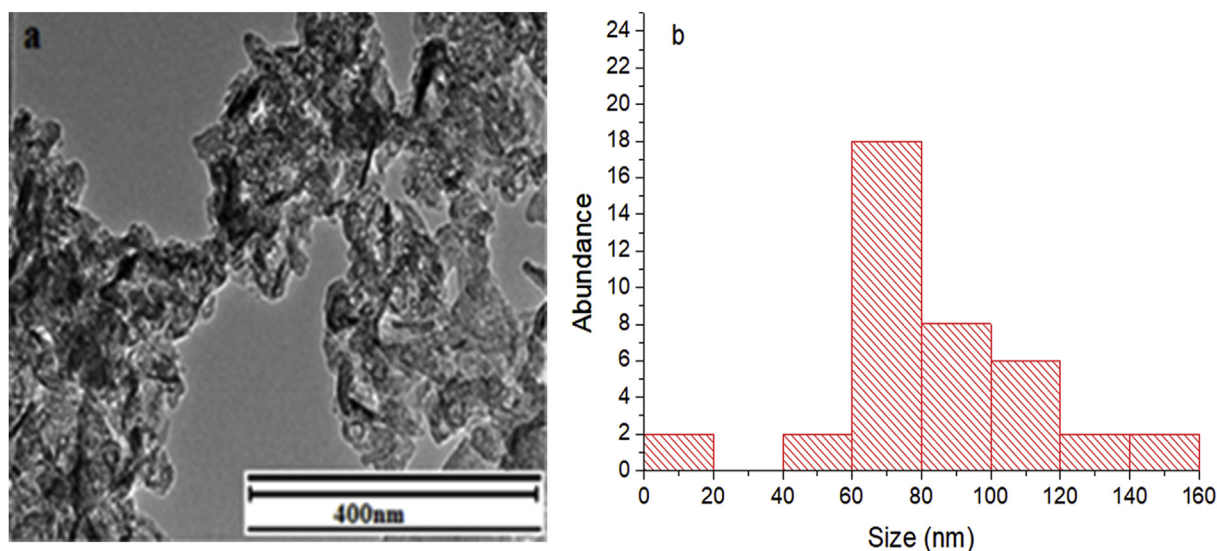


Fig. 5. TEM image (a) and particle size distribution (b) of chemically purified cellulose extracted from sugarcane bagasse.

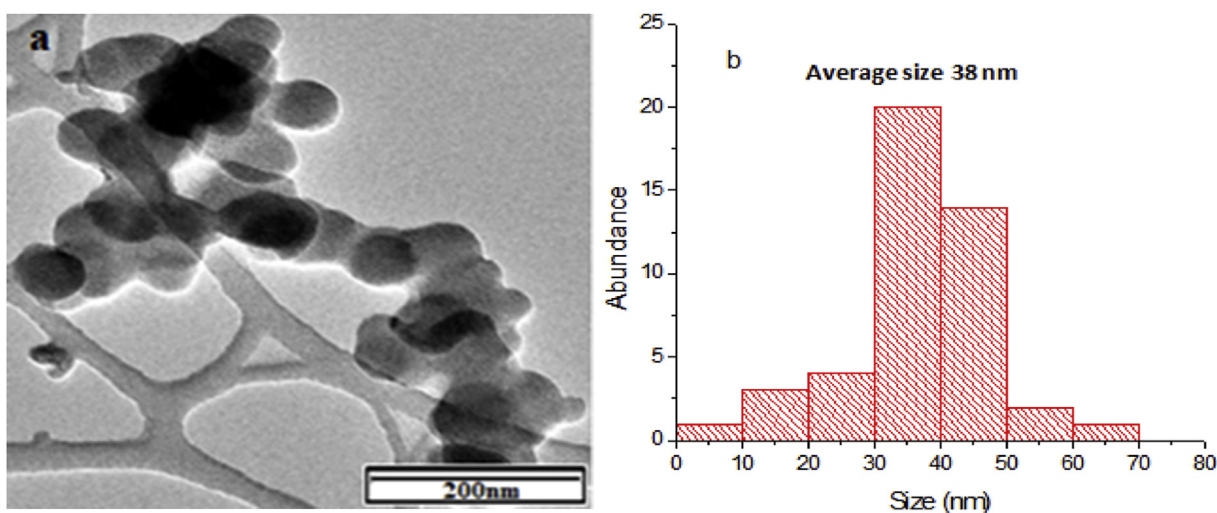


Fig. 6. TEM image (a) and particle size distribution (b) of cellulose nanocrystals prepared from the extracted chemically purified cellulose.

undergone Ostwald ripening. The CNCs on the other hand have a spherical shape with little agglomeration observed as compared to other studies. This agglomeration is attributed to the surface ionic charge that made the crystallites get stacked together due to acid hydrolysis process (Liu et al., 2010). The observed agglomeration may also be due to TEM sample preparation process once the dispersing medium was removed (Pires et al., 2013) though this agglomeration was seen to reduce significantly for the CNCs. The cellulosic chains are known to have hydrogen bonds and also some hydrophilic interaction between the chains which might also be responsible for the observed agglomeration (Kumar et al., 2014).

In other similar studies, Rosli et al. (2013), prepared CNCs from *Agave angustifolia* fiber that showed needle like structure consisting of some fibrils and some aggregates. These fibrils had an average diameter of 10 nm with a length of 310 nm Chieng et al. (2017), also observed agglomerated crystals of cellulose from Oil palm mesocarp which had an approximate diameter of 5 nm. Nanocellulose was also prepared in another study by acid hydrolysis of isolated cellulose from sugarcane bagasse using varied concentrations of sulfuric acid (Wulandari et al., 2016). He equally observed agglomerated spherical shaped nanocellulose having a diameter of about 197 nm. In most studies the agglomeration was attributed to the surface ionic charges which made

the crystals to stick together after the hydrolysis process.

#### 4. Conclusion

The study confirms cellulose can be obtained from sugarcane bagasse. The removal of non-cellulosic compounds can be enhanced by the use of nitric acid during chemical treatment and washing with acetone after sulfuric acid hydrolysis. An increase in crystallinity was observed for the nanocrystals which indicated the exposure of the crystalline phase after successful elimination of the lignin and hemicelluloses. The particle size greatly reduced in diameter after the acid hydrolysis of cellulose as observed by TEM and this is an indicator in improved properties of the CNCs. The results obtained herein suggest that SCB which is a menace in all the sugar factories can be utilized effectively for several other aspects since they possess the advantages of being sustainable and biodegradable.

#### Declarations

##### Author contribution statement

Wesley Nyaigoti Omwoyo: Conceived and designed the experiments;

Wrote the paper.

Evans K Suter: Performed the experiments.

Nathan Nyaigoti Oyaro: Analyzed and interpreted the data.

Makwena J Moloto: Contributed reagents, materials, analysis tools or data.

#### Funding statement

This research did not receive any specific grant from funding agencies in the public, commercial, or not-for-profit sectors.

#### Competing interest statement

The authors declare no conflict of interest.

#### Additional information

No additional information is available for this paper.

#### Acknowledgements

The authors wish to thank the Department of Chemistry, Vaal University of Technology for providing the necessary laboratory space, chemicals and equipment for the success of the work. Dr. Pierre Mubiayi of the University of Witwatersrand is also appreciated for the TEM analysis.

#### References

- Ahmed, M., Azizi, S., Alloin, F., Dufresne, A., 2005. Review of recent research into cellulosic whiskers, their properties and their application in nanocomposite field. *Biomacromolecules* 6, 612–626.
- Alemdar, A., Sain, M., 2008. Isolation and characterization of nanofibers from agricultural residues – wheat straw and soy hulls. *Bioresour. Technol.* 99, 1664–1671.
- Bledzki, A.K., Mamun, A.A., Volk, J., 2010. Composites: part A Physical, chemical and surface properties of wheat husk, rye husk and soft wood and their polypropylene composites. *Composites Part A* 41 (4), 480–488.
- Brebu, M., Vasile, C., 2010. Thermal degradation of lignin – a review. *Cellul. Chem. Technol.* 44 (9), 353–363.
- Chieng, B., Syn, L., Nor, I., Yoon, T., Yuet, L., 2017. Isolation and characterization of cellulose nanocrystals from Oil palm Mesocarp fiber. *Polymers* 9, 355–366.
- Costa, L., Amanda, F., Fabiano, P., Janice, D., 2015. Extraction and characterization of cellulose nanocrystals from corn stover. *Cellul. Chem. Technol.* 49 (2), 127–133.
- Faruk, O., Bledzki, A.K., Fink, H., Sain, M., 2012. Progress in polymer science biocomposites reinforced with natural fibers: 2000 – 2010. *Prog. Polym. Sci.* 37 (11), 1552–1596.
- Jacobsen, S.E., Wyman, C.E., 2000. Cellulose and hemicellulose hydrolysis models for application to current and novel pretreatment processes. *Appl. Biochem. Biotechnol.* 84 (86), 81–96.
- Johar, N., Ahmad, I., Dufresne, A., 2012. Extraction, preparation and characterization of cellulose fibres and nanocrystals from rice husk. *Ind. Crops Prod.* 37 (1), 93–99.
- Klemm, D., Heublein, B., Fink, H., Bohn, A., 2005. Polymer science Cellulose: fascinating biopolymer and sustainable raw material. *Cellulose: Chemistry and applications. Angew. Chem. Int. Ed.* 44, 3358–3393.
- Kumar, A., Negi, Y.S., Choudhary, V., Bhardwaj, N.K., 2014. Characterization of cellulose nanocrystals produced by acid-hydrolysis from sugarcane bagasse as agro-waste. *Journal of Materials Physics and Chemistry* 2 (1), 1–8.
- Lavoine, N., Desloges, I., Dufresne, A., Bras, J., 2012. Microfibrillated cellulose – its barrier properties and applications in cellulosic materials: a review. *Carbohydr. Polym.* 90 (2), 735–764.
- Li, R., Fei, J., Cai, Y., Li, Y., Feng, J., Yao, J., 2009. Cellulose whiskers extracted from mulberry: a novel biomass production. *Carbohydr. Polym.* 76 (1), 94–99.
- Liu, H., Liu, D., Yao, F., Wu, Q., 2010. Bioresource Technology Fabrication and properties of transparent polymethylmethacrylate/cellulose nanocrystals composites. *Bioresour. Technol.* 101 (14), 5685–5692.
- Liu, R., Yu, H., Huang, Y., 2005. Structure and morphology of cellulose in wheat straw structure and morphology of cellulose in wheat straw. *Cellulose* 12, 25–34.
- Lu, P., Hsieh, Y., 2010. Preparation and properties of cellulose nanocrystals: rods, spheres, and network. *Carbohydr. Polym.* 82 (2), 329–336.
- Masayi, N., Netondo, G., 2012. Effects of sugarcane farming on diversity of vegetable crops in Mumias Division, Western Kenya. *Int. J. Biodivers. Conserv.* 4 (13), 515–524.
- Mashego, D.V., 2016. Preparation, Isolation and Characterization of Nanocellulose from Sugarcane Bagasse. MSc thesis. Durban University of Technology, South Africa.
- Moon, R.J., Martini, A., Nairn, J., Simonsen, J., Youngblood, J., 2011. Cellulose nanomaterials review: structure, properties and nanocomposites. *Chem. Soc. Rev.* 40, 3941–3994.
- Nie, S., Zhanga, C., Zhanga, Q., Zhanga, K., Zhanga, Y., Tao, P., Wanga, S., 2018. Enzymatic and cold alkaline pretreatments of sugarcane bagasse pulp to produce cellulose nanofibrils using a mechanical method. *Ind. Crops Prod.* 124, 435–441.
- Otieno, J.D., 2015. Productivity of Sugar Factories in Kenya. MSc thesis. University of Nairobi, Kenya.
- Pasquini, D., Morais, E., Aprígio, A., Naceur, M., Dufresne, A., 2010. Extraction of cellulose whiskers from cassava bagasse and their applications as reinforcing agent in natural rubber. *Ind. Crops Prod.* 32 (3), 486–490.
- Pires, W., Neto, F., Alves, H., Oliveira, N., Pasquini, D., 2013. Extraction and characterization of cellulose nanocrystals from agro-industrial residue – soy hulls. *Ind. Crops Prod.* 42, 480–488.
- Plackett, D., 2010. Microfibrillated cellulose and new nanocomposite materials: a review. *Cellulose* 17, 459–494.
- Reddy, N., Yang, Y., 2005. Structure and properties of high quality natural cellulose fibers from cornstalks. *Polymer* 46, 5494–5500.
- Rosa, M.F., Medeiros, E.S., Malmonge, J.A., Gregorski, K.S., Wood, D.F., Mattoso, L.H.C., Imam, S.H., 2010. Cellulose nanowhiskers from coconut husk fibers: effect of preparation conditions on their thermal and morphological behavior. *Carbohydr. Polym.* 81 (1), 83–92.
- Rosli, N.A., Ahmad, I., Abdullah, I., 2013. Isolation and characterization of cellulose nanocrystals from *Agave angustifolia* fibre. *Bioresources* 8 (2), 1893–1908.
- Tao, P., Zhanga, Y., Wua, Z., Liaoa, X., Niea, S., 2019. Enzymatic pretreatment for cellulose nanofibrils isolation from bagasse pulp: transition of cellulose crystal structure. *Carbohydr. Polym.* 214, 1–7.
- Wang, B., Sain, M., 2007. Isolation of nanofibers from soybean source and their reinforcing capability on synthetic polymers. *Compos. Sci. Technol.* 67, 2521–2527.
- Wulandari, W., Rochliadi, A., Arcana, M., 2016. Nanocellulose prepared by acid hydrolysis of isolated cellulose from sugarcane bagasse. *Material Sci. and Eng.* 107, 1–7.
- Yang, H., Yan, R., Chen, H., Zheng, C., Lee, D.H., Liang, D.T., 2006. In-depth investigation of biomass pyrolysis based on three major Components: hemicellulose, cellulose and lignin. *Energy Fuels* 20, 388–393.
- Zuluaga, R., Luc, J., Cruz, J., Vélez, J., Mondragon, I., Gañán, P., 2009. Cellulose microfibrils from banana rachis: effect of alkaline treatments on structural and morphological features. *Carbohydr. Polym.* 76 (1), 51–59.